Physics Letters B 779 (2018) 348–352

Contents lists available at ScienceDirect

Physics Letters B

www.elsevier.com/locate/physletb

The string soundscape at gravitational wave detectors

Isabel Garcia Garcia [a,b], Sven Krippendorf [b,c,*], John March-Russell [b]

[a] Merton College, Merton Street, Oxford OX1 4JD, UK
[b] Rudolf Peierls Centre for Theoretical Physics, University of Oxford, 1 Keble Road, Oxford OX1 3NP, UK
[c] Arnold Sommerfeld Center for Theoretical Physics, LMU, Theresienstr. 37, 80333 München, Germany

ARTICLE INFO

Article history:
Received 11 December 2017
Received in revised form 7 February 2018
Accepted 11 February 2018
Available online 19 February 2018
Editor: A. Ringwald

Keywords:
Gravitational waves from phase transitions
String phenomenology

ABSTRACT

We argue that gravitational wave signals due to collisions of ultra-relativistic bubble walls may be common in string theory. This occurs due to a process of post-inflationary vacuum decay via quantum tunnelling. Though we study a specific string construction involving warped throats, we argue that our conclusions are more general. Many such transitions could have occurred in the post-inflationary Universe, as a large number of throats with exponentially different mass scales can be present in the string landscape, leading to several signals of widely different frequencies – a *soundscape* connected to the landscape of vacua. Detectors such as aLIGO/VIRGO, LISA, and pulsar timing observations with SKA and EPTA have the sensitivity to detect such signals. A distribution of primordial black holes is also a likely consequence, though reliable estimates of masses and their abundance require dedicated numerical simulations, as do the fine details of the gravitational wave spectrum due to the unusual nature of the transition.

1. Introduction

The recent direct detection of gravitational waves (GWs) [1,2] opens a new mode of physical exploration. Although the potential of GW detectors to study astrophysical objects is well-known [3], their potential for exploring Beyond-the-Standard-Model physics is still in a relative infancy. Prime examples studied so far include the physics of inflation [4–8], the presence of strongly first order thermal phase transitions [9–15], and the possibility of probing the existence of axions [16].

We argue that GW detectors provide a powerful tool to interrogate the nature of short-distance physics, particularly string theory, in a way unrelated to inflation: specifically, GW signals from *post-inflationary* vacuum decay are a natural feature of (at least) the type IIB string landscape. In particular it is well known that type IIB flux compactifications can contain a large number of highly warped throats [17–21], with physics related to that of Randall–Sundrum models [22,23] (see Fig. 1). Importantly for our purposes, a throat can present a metastable vacuum in which supersymmetry (SUSY) is locally broken, along with a locally-SUSY-preserving vacuum [24], to which it eventually decays.

Here we explore early-Universe vacuum decay taking place via zero-temperature quantum nucleation of bubbles of true, locally-SUSY-preserving, vacuum within a given throat, and argue that the resulting ultra-relativistic bubble wall collisions can lead to an *observable* stochastic 'background' of GWs. The peak frequency sensitively depends on the throat characteristics, most of all on the gravitational warp factor $w_{IR} \ll 1$, which sets the relation between the infra-red energy scale of the throat tip and the string scale M_s. Since a large number of throats with exponentially different warp factors can be present in the string landscape [25], GW signals with very different frequencies can be produced – a *soundscape* of possible signals that can be potentially discovered by detectors such as aLIGO [26] and LISA [27], and pulsar timing arrays [28,29]. Larger compactification volumes and smaller w_{IR} both shift the frequency towards smaller values, making pulsar timing optimal for probing large volume and/or strongly warped scenarios.

Ultra-relativistic bubble wall collisions can also produce primordial black holes (pBHs) [30–34]. Both this process and the GW spectrum beyond the frequency peak, are sensitive to the peculiarities of the bubble wall and vacuum decay dynamics applying in our case, which are different from those of both thermal phase transitions and previous studies of inflation-terminating quantum tunnelling vacuum decay. A detailed understanding of both the high-frequency features of the GW signal, and the mass spectrum of pBHs produced, requires dedicated numerical simulations, a study which is beyond the scope of this work. If, however, the

* Corresponding author.
E-mail addresses: isabel.garciagarcia@physics.ox.ac.uk (I. Garcia Garcia), sven.krippendorf@physik.lmu.de (S. Krippendorf), jmr@thphys.ox.ac.uk (J. March-Russell).

https://doi.org/10.1016/j.physletb.2018.02.028

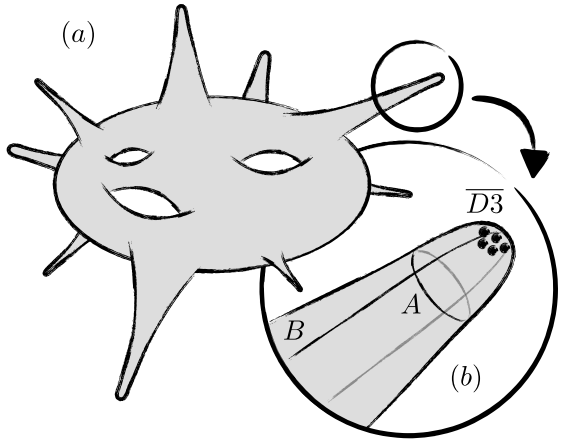

Fig. 1. (a) Cartoon of a type IIB flux compactification with a large number of throats, some of Klebanov–Strassler type [35]. (b) Close-up of a Klebanov–Strassler throat with 3-form flux quanta on the A- and B-cycles. The fluxes lead to a tip warp factor w_{IR}. In the locally SUSY-breaking false vacuum $\overline{D3}$ branes are localized at the tip [24].

production of pBHs is highly efficient, and has a mass distribution extending above $\simeq 10^9$ g, then the maximum amplitude of GWs observable today can be constrained. On the other hand, the possible production of pBHs in those mass ranges where they may account for (part of) the dark matter provides further motivation for detailed studies of the rich physics of the string soundscape.

2. False vacuum decay

2.1. Outline of early universe history

After inflation, the visible sector, i.e. the Standard Model plus other states in significant thermal contact with it, gets reheated to a temperature T_{rh}.[1] On the other hand, hidden sectors such as those living at the end of highly warped throats, may not be equally reheated and, in general, one expects many to be left at temperatures $T \ll T_{rh}$. In the following we take, for simplicity, the throat sector under consideration to be at temperature $T_{th} = 0$, although strictly speaking all required is that T_{th} is much smaller than all mass scales present in the problem. We note that this $T_{th} = 0$ choice is a self-consistent assumption, since the infra-red dynamics of a throat are sufficiently sequestered from the dynamics of the rest of the compactification to ensure that a hot thermal Standard Model sector localized elsewhere in the compactification interacts only feebly with the infra-red degrees of freedom of the throat [36,37].[2]

The relevant throat sector remains in a metastable vacuum so long as $\Gamma/H(T)^4 \ll 1$, where Γ is the decay rate per unit volume, and $H(T)$ is the Hubble rate, dependent on the *visible* sector temperature T. Γ is independent of temperature since $T_{th} = 0$. Only when $\Gamma/H(T)^4 \approx 1$ does the decay occur. Throughout, we assume that the visible sector radiation energy density, $\rho_{rad}(T)$, dominates over the false vacuum energy density, so that a second inflationary phase with potentially disastrous consequences [43,44] never takes place. Thus $\alpha(T) \equiv \rho_{vac}/\rho_{rad}(T) < 1$ for all temperatures of interest, ensuring a radiation dominated Universe.[3]

Both the SM temperature at nucleation, T_n, and the bubble properties, depend on the microphysics of our specific model to which we now turn. Readers primarily interested in the resulting GW phenomenology may jump to the next sub-section.

2.2. Metastable throats

Kachru et al. [24] considered the dynamics of p anti-$D3$ branes ($\overline{D3}$) in a Klebanov–Strassler throat [35]. In this so-called conifold geometry, which is topologically equivalent to $S^3 \times S^2 \times \mathbb{R}$, M units of so-called RR 3-form flux pierce the A-cycle of the conifold, whereas K units of so-called NSNS 3-form flux pierce the dual B-cycle. The A-cycle corresponds to the S^3 of the conifold, and the B-cycle extends into the bulk of the geometry when embedded into a compact manifold, as we illustrate schematically in Fig. 1. These fluxes result in a tip warp factor $w_{IR} \sim \exp(-2\pi K/3Mg_s)$ where g_s is the string coupling [17]. Ignoring back-reaction both local to the throat and arising from other distant parts of the compactification, in [24] it was argued that if the ratio p/M was smaller than a certain critical value $r_c = (\pi - 3 + b_0^4)/(4\pi) \approx 0.08$ then the system features a metastable vacuum in which SUSY is locally broken by the $\overline{D3}$-branes. Decay to the true SUSY-preserving vacuum, with no $\overline{D3}$-branes, $(M - p)$ $D3$-branes, and $(K - 1)$ NSNS flux quanta could only take place quantum mechanically, or through a thermal transition.

In the metastable vacuum, the system is not well described in terms of individual $\overline{D3}$ branes, but rather as an NS5 brane (a 5-dimensional object). This NS5 brane has 3 non-compact spatial dimensions, the remaining 2 being wrapped around an S^2 contained in the S^3 of the conifold geometry. The position of this S^2 within the S^3 is described by an angular variable ψ. The state of the system can then be encapsulated by the dynamics of a scalar field ψ, initially in a false vacuum $\psi_{fv} \in [0, \pi/4)$, and whose value in the true vacuum is $\psi_{tv} = \pi$ [24]. The Lagrangian describing this system (setting $M_s \equiv 1/\sqrt{\alpha'} = 1$ and in red-shifted units, so hiding the warp factor w_{IR}) is [24]

$$\mathcal{L} \approx \frac{\mu_3 M}{g_s}\left(-V_2(\psi)\sqrt{1-\partial_\mu\psi\,\partial^\mu\psi} + \frac{1}{2\pi}(2\psi - \sin 2\psi)\right), \tag{1}$$

where

$$V_2(\psi) = \frac{1}{\pi}\sqrt{b_0^4 \sin^4\psi + (\pi\frac{p}{M} - \psi + \frac{1}{2}\sin 2\psi)^2}\,, \tag{2}$$

with $\mu_3 = (2\pi)^{-3}$ and $b_0^2 \approx 0.93266$. When $p/M < r_c$ the potential has a local minimum below $\psi = \pi/4$, while for $p/M \geq r_c$ only the minimum at $\psi_{tv} = \pi$ exists. (We refer the reader to [24] for further details.)

Typical values of the flux quanta are $K, M \lesssim \mathcal{O}(10^2)$ [17,46], and a string coupling $g_s \ll 1$ is required for the validity of this effective action, with $g_s \sim \mathcal{O}(10^{-2})$ appropriate to accommodate the correct SM couplings [47]. For illustration, we take $M = 10^2$ and $g_s = 0.03$ in this work. Since we consider different values of the warp factor w_{IR}, this amounts to varying K.

Note that the local non-compact set-up of [24], used in this letter, suffers from back-reaction of $\overline{D3}$-branes on the geometry.

[1] In this work, we assume $T_{rh} \gtrsim 4$ MeV so that Big Bang Nucleosynthesis can proceed undisrupted, although we note that this assumption can be relaxed within more general early Universe histories.

[2] The case $T_{th} \neq 0$ would lead to *thermally assisted* quantum tunnelling decay, or a *purely thermal transition* if T_{th} is high enough, similar to the Randall–Sundrum case [38–42].

[3] A period of matter domination (see [45] for an overview), taking place either during or after the transition, but before the start of Big Bang Nucleosynthesis, is a well motivated possibility, and leads to interesting variant phenomenology.

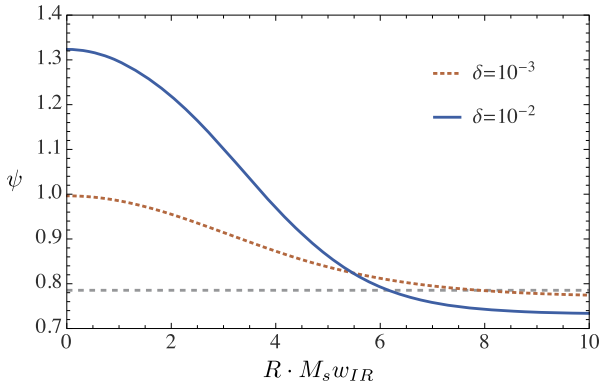

Fig. 2. Profile of a critical bubble at nucleation as a function of $\tilde{R} \equiv R \cdot M_s w_{IR}$, for two different values of δ. In both cases, a thick-wall profile occurs. The dashed line is $\psi = \pi/4$, the asymptotic value, as $\delta \to 0$, of the field in the false vacuum.

This issue has led to a long-standing debate [48–60], but as of now there is no definitive full string theory calculation on this point. Here we assume that the point of view of [60] is appropriate, and hence that the local back-reaction will not change the *qualitative* features of this system but only small quantitative changes will occur, such as a somewhat smaller value of r_c.

2.3. Bubble nucleation

Unlike the authors of [24], we focus on the case $p/M \lesssim r_c$, close to the regime of classical instability. We stress that our consideration of one or more throats close to such regime is not unreasonable: given the large number of throats typically present in the type IIB landscape, *some* of them can find themselves in this near-to-critical situation. In order to parametrize the system's deviation from criticality, we introduce a parameter δ, defined as

$$p/M \equiv r_c(1-\delta)\,, \qquad \text{with} \qquad 0 < \delta \ll 1\,. \tag{3}$$

Following Coleman [61], the decay rate per unit volume can be written as $\Gamma \sim m^4 e^{-B}$. B is defined as $B = S[\psi_B] - S[\psi_{fv}]$, where ψ_B is the field configuration, the so-called *bounce* solution, that extremizes the Euclidean action, and ψ_{fv} refers to the static false vacuum configuration. The mass scale m is sufficiently well approximated by the curvature around the barrier, and we find $(m/M_s)^4 \simeq 17 w_{IR}^4 \delta$. Moreover, since the metastable vacuum is close to classical instability, the vacuum energy density, ρ_{vac}, is much larger than the barrier height, and thus one should expect the bubbles at nucleation to show a thick-wall profile, rather than a thin-wall profile as considered in [24] for the case $p/M \simeq 0$ (see Fig. 2). In this regime, $\psi_B(\tilde{R})$ will change slowly with $\tilde{R}$ (here $\tilde{R} \equiv R \cdot M_s w_{IR}$, with R being the SO(4)-invariant Euclidean radius), an observation that allows the bounce equation to be simplified as

$$\frac{d^2\psi}{d\tilde{R}^2} + \frac{3}{\tilde{R}}\frac{d\psi}{d\tilde{R}} \simeq \frac{\pi V_2(\psi)' - 1 + \cos(2\psi)}{\pi V_2(\psi)}\,, \tag{4}$$

which can be solved numerically using the undershoot/overshoot method. We use [62] to this end. Once the bounce solution $\psi_B(\tilde{R})$ has been obtained, numerical evaluation of the bounce action B becomes straightforward. We find

$$B = 2\pi^2 \mu_3 b_0^4 g_s M^3 f(\delta) \tag{5}$$

$$\simeq 36\,\frac{g_s}{0.03}\left(\frac{M}{10^2}\right)^3 \frac{f(\delta)}{f(10^{-3})} \tag{6}$$

where $f(\delta) \simeq 0.38\ \delta^{1/2} + 6.0\ \delta$ for $\delta \simeq 10^{-4}$ to 10^{-2}.

Some comments are in order. First, gravitational effects [63] are unimportant for the nucleation, as in the region of parameter space we consider the critical radius of the bubbles at the time of nucleation, R_c, always satisfies $R_c \ll H(T_n)^{-1}$. Secondly, since the decay takes place when $\Gamma/H(T)^4 \approx 1$, one does not need to worry about counting of negative fluctuation modes of the bounce solution [64], since in this regime it is a theorem that one and only one negative mode is present and therefore the Euclidean bounce solution is guaranteed to correctly compute the false vacuum decay [65].[4] Thirdly, one might question our entitlement to vary δ essentially continuously: since p refers to the number of $\overline{D3}$ branes at the tip of the throat, and M to the units of RR flux, one would think that only discrete values of their ratio, and thus discrete values of δ, can be considered. However, small, but important corrections appear when embedding the local setup of [24] into a complete, global compactification manifold depending on the suppression of couplings between local and global modes (sequestering) [66,67]. For us, this dependence of local parameters such as w_{IR} and especially δ on bulk properties, including the enormously large number of distant flux values, effectively produces a very finely grained discretum [68–70], justifying our choice of varying δ continuously.

3. Gravitational waves

3.1. Expansion of bubbles

At nucleation, the bounce solution implies the critical bubbles are spherical and at rest.[5] Quickly after nucleation they become ultra-relativistic, with an effectively thin-wall profile. As we consider a $T_{th} = 0$ tunnelling process, production of GWs arises dominantly from bubble collisions: effects like sound-waves or turbulence in the thermal plasma, which modify the GW spectrum in the case of thermal transitions [15] are, to a good approximation, not present (the only thermal plasma present is the SM plasma, and this is only feebly coupled to the throat sector). Unlike most thermal transitions where the temperatures at bubble nucleation and collision are very close to each other, in our situation this is not the case. Bubbles of critical size are nucleated at temperature T_n (or time t_n), when $\Gamma/H(t_n)^4 \approx 1$, and since the radius of this critical bubbles is $R_c \ll H(t_n)^{-1}$, we can treat them as point-like. Bubbles then expand and, within a radiation dominated Universe, collide at a time $\Delta t \approx 1.6 t_n$ after nucleation. This translates into a temperature at collision $T_c = T_n\sqrt{t_n/t_c} \approx 0.62 T_n$, and thus $\alpha_n \approx 0.15\alpha_c$, where $\alpha_{n,c} \equiv \alpha(T_{n,c})$.

3.2. Collision of bubbles

Emission of GWs occurs when bubbles collide, leading to a stochastic background of GWs. Assuming a radiation dominated Universe during and immediately after the decay, we can estimate the present frequency peak of the signal as [14,73]

$$f_0 \sim 10^{-5}\ \text{Hz}\left(\frac{g_*(T_c)}{100}\right)^{\frac{1}{6}}\left(\frac{T_c}{100\ \text{GeV}}\right)\frac{1}{t_* H(T_c)}\,, \tag{7}$$

where t_* refers to the duration of the transition. Given that $\Delta t \sim H(T_n)^{-1}$, we expect $t_* H(T_c) = \mathcal{O}(1)$, and so we take $t_* H(T_c) \approx 1$

[4] As an aside we comment that this feature is not assured in the much different parameter regime considered in [24], so it is not clear if in [24] a *physical* decay rate has been calculated or not.

[5] We note that theses statements regarding the nucleated bubbles are accurate up to corrections of order $1/\sqrt[3]{B}$ [71,72]. This is a $SO(2,1)$-symmetry-breaking effect in the case of two bubbles. A full, correct treatment of the high-frequency part of the GW spectrum, and the details of pBH production would require inclusion of these effects.

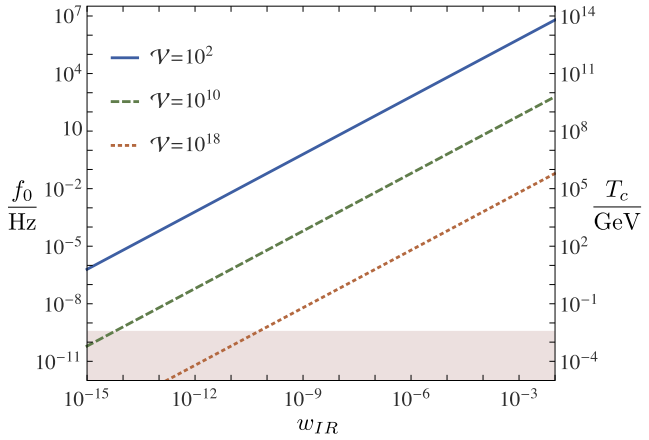

Fig. 3. Approximate peak frequency of the GW signal as a function of the warp factor w_{IR}, keeping $\alpha_c = 1$ fixed and for 3 different 6D compactification volumes $\mathcal{V}$ (in units of $(2\pi l_s)^6$, where $l_s \equiv \sqrt{\alpha'}$). For illustration, we fix $M = 10^2$ and $g_s = 0.03$. The shaded region indicates $T_c < 4$ MeV (inaccessible if $\alpha_c \sim 1$ for a standard cosmological history if Big Bang Nucleosynthesis is to proceed undisrupted).

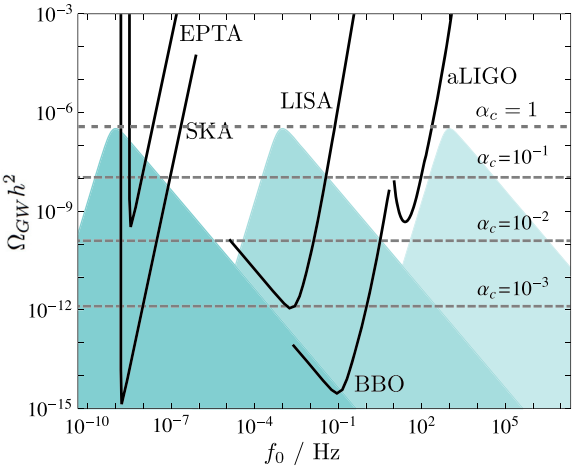

Fig. 4. Colored regions correspond to the approximate profile of the stochastic GW background due to bubble collisions, together with sensitivity curves of different experiments. For illustration, we choose three different frequency peaks: $f_0 = 10^{-9}, 10^{-3}$ and 10^3 Hz, all within the reasonable range of frequencies expected (see Fig. 3), and $\alpha_c = 1$. Dashed lines indicate how the position of the peak amplitude would decrease for smaller values of α_c. For a given frequency peak, the shape of the spectrum for frequencies much below the peak frequency is dictated by causality, while the exact spectrum shape in the region around and above the peak frequency is *sensitive to details of the specific dynamics of the transition and requires dedicated numerical simulation* (as illustration we show the *standard* expectation for the GW spectrum in this peak-and-above frequency region with turbulence and sound wave contributions removed, as this likely roughly approximates the true high-f spectra ignoring fine details).

for illustration in Fig. 3 and Fig. 4, albeit an accurate determination of t_* would require numerical simulations. Notice that since Γ is independent of the temperature of the thermal bath, only a few large bubbles will be present at the time of collision, and so we expect t_* to be of order the time these bubbles take to grow until they meet each other. Also, we note that although the dominant collision is between ultra-relativistic bubbles of size $\sim H(t_n)$ there are $\mathcal{O}(10\text{–}100)$ small, semi-relativistic, thick-walled bubbles with which each large bubble additionally collides. This is unlike what occurs in the case of a thermal first order transition, where the strong dependence of Γ on the temperature results in many bubbles being nucleated once the critical temperature of the transition is reached.

Fig. 3 shows the frequency of our estimate of the peak GW signal as a function of the tip warp factor w_{IR}, for $\alpha_c = 1$. The frequency of this signal can span virtually the whole range of parameter space that will be explored by current and future GW detectors, including the high-frequency range, $\gtrsim 30$ kHz, where radically new technologies are necessary, but where conventional astrophysical foregrounds are absent. Large values of the compactification volume $\mathcal{V}$ shift the peak signal frequency towards lower values. The value of δ corresponding to the region of parameter space considered in Fig. 2 ranges from 10^{-3} in the high frequency region to 10^{-2} at low frequencies, well within the range of validity of our approximations.

Given the unusual nature of the transition, and of the ψ-field kinetic term (see Eq. (1)), a precise expression for the energy density in GWs observed today, as a function of frequency, requires numerical simulations. However, energetic considerations suggest the peak amplitude is likely well approximated by the usual expression for ultra-relativistic bubble wall collisions [73–75]:

$$\Omega_{GW}h^2(f_0) \sim 10^{-6}\left(\frac{\alpha_c}{1+\alpha_c}\right)^2\left(\frac{10^2}{g_*}\right)^{\frac{1}{3}}(t_* H(T_c))^2 \ . \tag{8}$$

In Fig. 4, we show an approximation to the expected signals for three different values of the frequency peak. While the f_0^3 behavior below the peak is fixed by locality, the profile beyond the peak requires numerical simulations. In the present work, we have used the usual high-f_0 dependence purely for illustration [15].

4. Fate of the vacuum energy

The fraction of the vacuum energy density that converts into GWs is small, as can be seen from Eq. (8), and the remaining fraction must have a different fate. We now briefly outline some of the possibilities for this model dependent issue. To be general, we go beyond the possibilities for the Klebanov–Strassler throat to include all standard phenomenological possibilities which could arise in different throat geometries.

4.1. Dark radiation

If some throat degrees of freedom remain massless or very light (not present in the Klebanov–Strassler throat), and a fraction η_{DR} of the vacuum energy is transferred into these, they will behave as dark radiation, and constraints from bounds on the number of effective neutrino species apply. We find the contribution to ΔN_{eff} from massless throat states to be[6]

$$\Delta N_{eff}^{(th)} \approx 0.29\left(\frac{\eta_{DR}}{1}\right)\left(\frac{\alpha_c}{0.1}\right)\left(\frac{100}{g_*(T_c)}\right)^{\frac{1}{3}} \ . \tag{9}$$

Since the contribution to ΔN_{eff} from the SM is $\Delta N_{eff}^{(SM)} \approx 0.046$, and Planck has measured $\Delta N_{eff} \approx 0.15 \pm 0.23$ [76], even for $\eta_{DR} \approx 1$ and $\alpha_c \approx 0.1$, the prediction for $\Delta N_{eff}^{(th)}$ is small enough to be allowed and an observable GW signal is still present (see Fig. 4).

4.2. Primordial black hole production

Formation of pBHs takes place when ultra-relativistic bubbles collide [30–34], and so constraints due to evaporating pBHs can

[6] Note that $\Delta N_{eff}^{(th)}$ is independent of the number of massless throat degrees of freedom, unlike the case if the SM and the throat sector had been in thermal equilibrium.

apply [77]. Depending on the fraction of energy transferred into pBHs of a given mass m_{BH}, the strength of the GW signal over a certain range of frequencies could be constrained. More hopefully, production of pBHs with masses 10^{17}–10^{18} g, or over a broad range $m_{BH} > 10^{17}$ g, could account for a fraction of the dark matter, but formation of pBHs with masses $\sim 30 M_{\odot}$ (see [78]) does not seem possible within a radiation dominated Universe, albeit non-standard cosmological scenarios may allow this. Determining the extent to which pBH production occurs requires dedicated numerical simulations, taking into account the unusual transition and bubble dynamics.

4.3. Non-pBH dark matter

If sufficiently stable states exist in the throat sector, and a suitable fraction of ρ_{vac} is transferred to these, they could account for the DM [79–81]. Though this issue is highly model dependent, it provides an interesting possibility for dark matter model building with a candidate with features linked to those of the GW signal discussed in Section 3.

5. Conclusions

In this letter, we have shown how GW can be produced in the context of string theory, due to a process of vacuum decay linked to the landscape of vacua characteristic of string constructions. Our results show that the resulting GW signal can be within reach of current and future detectors, both in terms of frequency and strength, but also highlight the importance of developing new experiments that would cover the very high-frequency regime (above ≈ 30 kHz), where such a signal is possible but astrophysical backgrounds are absent.

This work emphasizes the importance of dedicated numerical simulations that take into account the characteristic 'stringy' features of such constructions, which is essential to determine the shape of the GW signal beyond the frequency peak, and the mass spectrum of pBHs produced. This is crucial in order to distinguish a signal of string origin from a conventional one.

Depending on the details of the specific string construction, a GW signal will typically be correlated with other observations, depending on the fate of the remaining vacuum energy not converted into GW. This may include dark radiation, a spectrum of pBHs, or non-BH dark matter. Although this issue is highly model dependent, it would also provide a way of distinguishing specific models.

Acknowledgements

We thank Joe Conlon and John Wheater for discussions. JMR thanks Sidney Coleman for his extraordinary guidance and friendship. SK's research was supported by the European Research Council under starting grant 'Supersymmetry Breaking in String Theory' (307605).

References

[1] B.P. Abbott, et al., Phys. Rev. Lett. 116 (6) (2016) 061102.
[2] B.P. Abbott, et al., Phys. Rev. Lett. 116 (24) (2016) 241103.
[3] P.D. Lasky, et al., Phys. Rev. X 6 (1) (2016) 011035.
[4] L.P. Grishchuk, Sov. Phys. JETP 40 (1975) 409.
[5] A.A. Starobinsky, JETP Lett. 30 (1979) 682.
[6] V.A. Rubakov, M.V. Sazhin, A.V. Veryaskin, Phys. Lett. B 115 (1982) 189.
[7] R. Fabbri, M.d. Pollock, Phys. Lett. B 125 (1983) 445.
[8] L.F. Abbott, M.B. Wise, Nucl. Phys. B 244 (1984) 541.
[9] E. Witten, Phys. Rev. D 30 (1984) 272.
[10] M.S. Turner, E.J. Weinberg, L.M. Widrow, Phys. Rev. D 46 (1992) 2384.
[11] A. Kosowsky, M.S. Turner, R. Watkins, Phys. Rev. Lett. 69 (1992) 2026.
[12] A. Kosowsky, M.S. Turner, R. Watkins, Phys. Rev. D 45 (1992) 4514.
[13] A. Kosowsky, M.S. Turner, Phys. Rev. D 47 (1993) 4372.
[14] M. Kamionkowski, A. Kosowsky, M.S. Turner, Phys. Rev. D 49 (1994) 2837.
[15] C. Caprini, et al., J. Cosmol. Astropart. Phys. 1604 (04) (2016) 001.
[16] A. Arvanitaki, et al., Phys. Rev. D 95 (4) (2017) 043001.
[17] S.B. Giddings, S. Kachru, J. Polchinski, Phys. Rev. D 66 (2002) 106006.
[18] M.R. Douglas, J. High Energy Phys. 05 (2003) 046.
[19] S. Ashok, M.R. Douglas, J. High Energy Phys. 01 (2004) 060.
[20] F. Denef, M.R. Douglas, J. High Energy Phys. 05 (2004) 072.
[21] A. Giryavets, S. Kachru, P.K. Tripathy, J. High Energy Phys. 08 (2004) 002.
[22] L. Randall, R. Sundrum, Phys. Rev. Lett. 83 (1999) 3370.
[23] L. Randall, R. Sundrum, Phys. Rev. Lett. 83 (1999) 4690.
[24] S. Kachru, J. Pearson, H.L. Verlinde, J. High Energy Phys. 06 (2002) 021.
[25] A. Hebecker, J. March-Russell, Nucl. Phys. B 781 (2007) 99.
[26] J. Aasi, et al., Class. Quantum Gravity 32 (2015) 074001.
[27] P. Amaro-Seoane, et al., Class. Quantum Gravity 29 (2012) 124016.
[28] P.E. Dewdney, et al., The square kilometre array, Proc. IEEE 97 (8) (2009) 1482–1496.
[29] M. Kramer, D.J. Champion, Class. Quantum Gravity 30 (2013) 224009.
[30] M. Crawford, D.N. Schramm, Nature 298 (1982) 538.
[31] S.W. Hawking, I.G. Moss, J.M. Stewart, Phys. Rev. D 26 (1982) 2681.
[32] H. Kodama, M. Sasaki, K. Sato, Prog. Theor. Phys. 68 (1982) 1979.
[33] I.G. Moss, Phys. Rev. D 50 (1994) 676.
[34] M.Yu. Khlopov, et al., arXiv:hep-ph/9807343.
[35] I.R. Klebanov, M.J. Strassler, J. High Energy Phys. 08 (2000) 052.
[36] S. Kachru, L. McAllister, R. Sundrum, J. High Energy Phys. 10 (2007) 013.
[37] S. Halter, B. von Harling, A. Hebecker, J. High Energy Phys. 02 (2010) 063.
[38] P. Creminelli, A. Nicolis, R. Rattazzi, J. High Energy Phys. 03 (2002) 051.
[39] L. Randall, G. Servant, J. High Energy Phys. 05 (2007) 054.
[40] B. Hassanain, J. March-Russell, M. Schvellinger, J. High Energy Phys. 10 (2007) 089.
[41] T. Konstandin, G. Nardini, M. Quiros, Phys. Rev. D 82 (2010) 083513.
[42] T. Konstandin, G. Servant, J. Cosmol. Astropart. Phys. 1112 (2011) 009.
[43] A.H. Guth, E.J. Weinberg, Nucl. Phys. B 212 (1983) 321.
[44] D. La, P.J. Steinhardt, Phys. Lett. B 220 (1989) 375.
[45] G. Kane, K. Sinha, S. Watson, Int. J. Mod. Phys. D 24 (08) (2015) 1530022.
[46] M. Kreuzer, H. Skarke, Adv. Theor. Math. Phys. 4 (2002) 1209.
[47] M. Cicoli, et al., J. High Energy Phys. 07 (2013) 150.
[48] R. Brustein, S.P. de Alwis, Phys. Rev. D 69 (2004) 126006.
[49] P. McGuirk, G. Shiu, Y. Sumitomo, Nucl. Phys. B 842 (2011) 383.
[50] I. Bena, M. Grana, N. Halmagyi, J. High Energy Phys. 09 (2010) 087.
[51] J. Blaback, U.H. Danielsson, T. Van Riet, J. High Energy Phys. 02 (2013) 061.
[52] I. Bena, et al., J. High Energy Phys. 02 (2015) 146.
[53] U.H. Danielsson, T. Van Riet, J. High Energy Phys. 03 (2015) 087.
[54] R. Kallosh, T. Wrase, J. High Energy Phys. 12 (2014) 117.
[55] B. Michel, et al., J. High Energy Phys. 09 (2015) 021.
[56] U.H. Danielsson, arXiv:1502.01234.
[57] E.A. Bergshoeff, et al., J. High Energy Phys. 05 (2015) 058.
[58] R. Kallosh, F. Quevedo, A.M. Uranga, J. High Energy Phys. 12 (2015) 039.
[59] I. Garcia-Etxebarria, F. Quevedo, R. Valandro, J. High Energy Phys. 02 (2016) 148.
[60] J. Polchinski, arXiv:1509.05710.
[61] S.R. Coleman, Phys. Rev. D 15 (1977) 2929.
[62] C.L. Wainwright, Comput. Phys. Commun. 183 (2012) 2006.
[63] S.R. Coleman, F. De Luccia, Phys. Rev. D 21 (1980) 3305.
[64] S.R. Coleman, Nucl. Phys. B 298 (1988) 178.
[65] H. Lee, E.J. Weinberg, Phys. Rev. D 90 (12) (2014) 124002.
[66] S. Kachru, et al., J. Cosmol. Astropart. Phys. 0310 (2003) 013.
[67] D. Baumann, et al., J. High Energy Phys. 11 (2006) 031.
[68] R. Bousso, J. Polchinski, J. High Energy Phys. 06 (2000) 006.
[69] J.L. Feng, et al., Nucl. Phys. B 602 (2001) 307.
[70] N. Arkani-Hamed, S. Dimopoulos, S. Kachru, arXiv:hep-th/0501082.
[71] J. Garriga, S. Kanno, T. Tanaka, J. Cosmol. Astropart. Phys. 1306 (2013) 034.
[72] J.R. Bond, J. Braden, L. Mersini-Houghton, J. Cosmol. Astropart. Phys. 1509 (09) (2015) 004.
[73] L. Leitao, A. Megevand, Nucl. Phys. B 905 (2016) 45.
[74] S.J. Huber, T. Konstandin, J. Cosmol. Astropart. Phys. 0809 (2008) 022.
[75] D.J. Weir, Phys. Rev. D 93 (12) (2016) 124037.
[76] P.A.R. Ade, et al., Astron. Astrophys. 594 (2016) A13.
[77] B.J. Carr, et al., Phys. Rev. D 81 (2010) 104019.
[78] S. Bird, et al., Phys. Rev. Lett. 116 (20) (2016) 201301.
[79] X. Chen, S.H.H. Tye, J. Cosmol. Astropart. Phys. 0606 (2006) 011.
[80] B. von Harling, A. Hebecker, J. High Energy Phys. 05 (2008) 031.
[81] A.R. Frey, R.J. Danos, J.M. Cline, J. High Energy Phys. 11 (2009) 102.